DEVELOPMENT OF AUTOMATED MOMENT TENSOR SOFTWARE AT THE PROTOTYPE INTERNATIONAL DATA CENTRE

Margaret Hellweg,[1] Douglas Dreger,[1] Barbara Romanowicz,[1] Jeffry Stevens[2]

University of California, Berkeley, Seismological Laboratory;[1] Science Applications International Corporation[2]

Sponsored by Defense Threat Reduction Agency

Contract No. DTRA01-00-C-0038

ABSTRACT

We are implementing the seismic moment tensor software used at the Berkeley Seismological Laboratory (BSL) for routinely monitoring earthquake strain release (Romanowicz *et al*., 1993; Pasyanos *et al*., 1996) on the test bed at the Center for Monitoring Research (CMR, formerly the Prototype International Data Centre (PIDC). The discrimination of nuclear explosions from naturally occurring earthquakes is difficult, particularly for moderate magnitude events. By providing a general representation of the seismic source, the moment tensor allows us to characterize its radiation in terms of isotropic and compensated linear vector dipole (CLVD) patterns in addition to the double couple radiation expected from typical tectonic earthquakes. The software package from BSL determines moment tensors for an event using two separate procedures: a complete waveform (CW) time-domain method as well as a spectral method applied to the surface wave (SW) recordings. During the past year, we have completed the implementation of the code package at CMR. This has involved major reworking of the waveform extraction package *mtisshell* to provide data pre-processing so that other programs such as the Seismic Analysis Code (SAC) or sapling ([a BSL processing module], Pasyanos, 1996) are no longer necessary. In addition, we have improved the estimation of signal-to-noise ratio for data used in the surface wave inversion to exclude noisy data that skews the inversion results. To illustrate the application, we present the inversion results from both methods for events with mb 5.4 in a test interval occurring between 19 July 1999 and 16 October 1999. The waveform data for input are taken from the very sparse network of the primary stations of the International Monitoring System (IMS), while the Greens functions (CW) are calculated using the IASPEI-91 velocity model and mode information for the SW code is derived from model 1066. We compare the results of both inversion methods with information given in the Harvard Centroid Moment Tensor (CMT) catalog and that in the moment tensor catalog of the US Geological Survey (USGS).

To improve its integration into the routine system, we are continuing to test and tune the procedure. Although the results for events in the test interval in some regions of the Earth are good, there are several regions where they could be improved. We show the effects of performing the inversions using theoretical information calculated on the basis of other Earth models. In addition, for selected events, we show how the addition of data from auxiliary stations improves the station coverage and thus the inversion results. On the basis of velocity structure and waveform data collected as part of the Advanced Concept Demonstration (ACD) centered on Lop Nor, we intend to investigate and demonstrate the advantages of Greens functions and mode calculations based on a regional velocity model and investigate the resolution of the two methods for moderate events, recorded well in the ACD region.

OBJECTIVE

Through moment tensor inversion, we can use broadband waveforms from modern broadband digital seismic stations to derive a robust estimate of source magnitude (M_w) for an event as well as information about its mechanism and its depth. In addition, the moment tensor results that are obtained using either primary stations of the International Monitoring System (IMS) or both primary and auxiliary stations will provide an important database of details about the seismic sources. This information will benefit other programmatic objectives such as the calibration of velocity and attenuation structure at both global and regional scales. Thus seismic moment tensors are a potentially powerful method for screening observed seismicity to identify anomalous events, those which are shallower than is typical and which have unusual, non-double couple radiation patterns (e.g. Patton 1988; Dreger and Woods, 2002). Such events may be flagged to be analyzed in greater detail. While previous work has demonstrated that moment tensors of nuclear explosions are different than those of tectonic earthquakes (Patton, 1988; Stump and Johnson, 1984; Vasco and Johnson, 1989), it was often difficult to resolve a purely isotropic source with regionally recorded long-period data (Patton, 1988). In contrast, recent experience indicates that anomalous radiation from nuclear explosions or non-tectonic seismic events may be identified with a relatively sparse network of broadband stations (e.g. Dreger and Woods, 2002; Dreger *et al*., 2000). These studies have identified significant deviation from double-couple type seismic radiation, but come up short in actually resolving the physical processes which give rise to the non-double-couple seismic radiation.

The moment tensor formalism was first developed more than 20 years ago (e.g. Mendiguren, 1977), and has been since applied successfully in various settings for the study and/or routine cataloguing of moderate to large earthquakes on the global scale, using either waveforms in the time-domain (e.g. Dziewonski *et al*., 1981) or surface-wave spectra in the frequency domain (e.g. Romanowicz, 1982; Romanowicz and Guillemant, 1984). When the signal-to-noise ratio is good, data from a single, three-component station are sufficient to obtain a moment tensor solution for a large, purely double-couple earthquake at teleseismic distances (Ekstrom *et al*., 1986). The same is true for regional distances, where a robust estimate of the seismic moment tensor of a moderate earthquake may be determined with data from a single, three-component station (e.g. Dreger and Helmberger, 1991; Fan and Wallace, 1991; Walter, 1993). For large earthquakes recorded teleseismically, relatively low frequency data can be used. In such cases, it is not necessary to know the propagation corrections with great accuracy. The use of standard 1D reference models of the Earth and, more recently, 3D models obtained from global tomography generally give acceptable solutions. More recently, as sparse regional broadband networks become more common, moment tensor inversion procedures have been adapted for application to smaller events observed at regional distances. In such cases, waves with periods between 15 and 40 s are used in the inversions. They are more sensitive to complex crustal structure, and propagation corrections must therefore be estimated more accurately using appropriate regional models. At U.C. Berkeley, we have developed and implemented two independent approaches for estimating the moment tensor of moderate earthquakes at regional distances (Romanowicz *et al*., 1993). They have been automated within the framework of our real-time program (Gee *et al*., 1996) to routinely provide reliable estimates of earthquake size, mechanism and depth in quasi-real time (Pasyanos *et al*., 1996).

In the time-domain moment tensor inversion procedure, the CW method, the complete long-period waveform from the initial P-wave through the surface wavetrain is used (Dreger and Romanowicz, 1994; Pasyanos *et al*., 1996; Fukuyama *et al*., 1998; Fukuyama and Dreger, 2000). This method functions quite well in a region as complex as California for monitoring seismicity 30 to 700 km from stations with only a few calibrated velocity models. One of the models we use describes the relatively fast wave propagation in the thick Sierra block, the second describes propagation through the relatively slow and thin California Coast Ranges (Pasyanos *et al*., 1996). Recently, a third model has been developed to improve results for events occurring offshore of Cape Mendocino (Tajima *et al*, 2000). While a satisfactory solution may often be derived using three-component data from a single station, in practice we use data from several stations to improve the azimuthal coverage of the focal sphere (Pasyanos *et al*., 1996).

The second moment tensor method used at U.C. Berkeley, the SW method, is a frequency-domain, surface wave approach, adapted from the two-step method of Romanowicz (1982). The use of surface waves, the largest of the regional phases, allows us to extend the analysis to smaller seismic events. For this procedure, calibrated fundamental-mode surface wave phase velocities between 10-60 sec period are used to calculate propagation corrections (Pasyanos *et al*., 1996). We are able to analyze events down to magnitude 3.5 using data from stations of the Berkeley Digital Seismic Network between 100 to 500 km from the epicenter. When azimuthal coverage is acceptable this method performs quite well.

The purpose of this project is to adapt and implement the two procedures in use at U.C. Berkeley for nuclear monitoring purposes. The initial goal for this software is the automatic determination of moment tensors on a global scale for events with magnitudes greater than M = 5.5. For a specific region, we will attempt to achieve reliable results for lower magnitudes through the use in the inversions of velocity structures adapted for the region as well as data from additional regional broadband stations. Later releases of the software will incorporate calibration information for several regions of interest, which will allow moment tensors to be determined for events with magnitudes greater than M ~ 4.

RESEARCH ACCOMPLISHED

We have developed and installed an automated processing system for the moment tensor package on the testbed at the Center for Monitoring Research (CMR). The flowchart in Figure 1 gives an overview of the automatically executed processing steps. For a given Julian date, events are selected for processing on the basis of information extracted from the database tables containing the reviewed event bulletin (REB). For our tests, we have chosen the interval from 19 July (day 200) to 16 October (day 290) 1999. If an event has a body-wave magnitude greater than 5.4 and depth shallower than 200 km, it is included in the processing. Table 1 lists the events in the testbed database with these characteristics. In addition to hypocentral information, the process automatically extracts from the database tables a list of the primary stations equipped with broadband sensors, which were used in producing the REB, along with event-station azimuths and distances. Several important events with REB $m_b < 5.4$ have been added to improve coverage, and to improve the testbed dataset for calibration purposes.

For those seismic stations, waveform data are extracted separately for the two inversion routines and preprocessed using the program *mtisshell*. The data intervals are chosen on the basis of group velocity. For the CW method, data lie within an interval having group velocities between 200 km/s and 2 km/s, and only includes stations located less than 5000 km from the epicenter. Data for the SW method are in an interval defined by group velocities between 4.5 km/s and 2 km/s. During the data extraction process, basic data quality tests are performed. If one or more components from a station has gaps in the selected interval or the interval for which data is present is shorter than requested, data from that station are excluded. For data to be used in the SW inversion, a second quality check is performed after they have been extracted. The power for the surface waves in the band of interest, usually between 100 s and 20 s, is compared with the power of the noise in an interval before the arrival of the P-wave from the event (group velocities between 200 km/s and 15 km/s). If the signal-to-noise ratio in power is lower than 100 for the Z, R or T components, data from that station are excluded from the inversion. The maps in Figure 2 show the primary stations, which provided waveform data for the events in the test. As is shown in Figure 1, the preprocessing depends on the inversion algorithm. For both methods, means and trends are removed from the data and they are then resampled to 1 sps. The instrument response is deconvolved and the records are rotated to directions radial (R) and transverse (T) to the event-station direction. While the data for the CW inversion is bandpass-filtered to extract the band to be used in the inversion, the filter limits for the SW data lie well outside the band of interest in order to exclude very long period noise without affecting the data to be inverted.

In addition to the waveform data, the CW method requires Greens function files for the fundamental fault orientations and movements (Dreger and Helmberger, 1991). The Greens functions used at U.C. Berkeley are calculated from the regional velocity models using *FKPROG*, a program for frequency-wavenumber calculation regional waveforms (Saikia, 1994). *FKPROG* treats the velocity model as a planar, not spherical structure, which is an acceptable assumption for near-regional distances of up to 700 km as in California. For the application of *FKPROG* to event-station distances up to 5000 km, as in the testbed implementation, the assumption is no longer valid. Initial tests of the CW method with Greens functions calculated directly from the radially symmetric iasp91 velocity model for the Earth (Kennett and Engdahl, 1991) were unsuccessful. Typically, time differences between phases in the Greens functions were too short to achieve good fits. We applied a flattening algorithm (Müller, 1973, Müller, 1977) to the iasp91 velocity model before calculating a new set of Greens functions. The agreement between the travel times in the Greens function synthetics for a given distance and the data for events at that distance from a station improved. Our analysis of the broadband waveform fits, and comparisons of derived moment tensor solutions with those reported by either Harvard or the USGS indicate that this flattening correction produces a robust set of Greens functions.

The upper map in Figure 2 shows the moment tensors calculated using the CW method and Greens functions based on a flattened iasp91 velocity model (blue) and on a flattened PREM velocity model (green, Dziewonski and Anderson, 1981). For comparison, the moment tensors given for these events in the Harvard CMT (brown) and USGS (red) catalogs are also shown. For events in the southwest Pacific Ocean, the moment tensors derived by the CW method differ from those given by both the Harvard and USGS catalogs. However, data for each of these events were only available for one primary station less than 5000 km from the epicenter, STKA. The solutions calculated by the CW method are consistent with the waveforms from this station. Were data from one or more other stations available, the additional constraints would probably improve the agreement with the standard catalogs. Figure 3A shows the moment tensor difference function (Pasyanos *et al*, 1996) comparing the results from the CW inversions using iasp91 and PREM Greens functions with Harvard CMT catalog moment tensors and with each other, while Figure 3B plots the ratios of the calculated moments to the catalogs' moments and between the different Greens functions. While there is some variation between the ratios of the moments, they cluster around 1. This indicates that the estimate of the moment using the CW method is reliable. On the whole, the agreement between the moment tensors from the CW method and Harvard CMT are not very good when described using the moment tensor difference function (Figure 3A).

The Hector Mine event (Origin ID 20595122, October 16, 1999) is a good example on which to investigate these differences. The map in Figure 4A shows the location of the Hector Mine event (star) and the primary stations of the network of the International Monitoring System (IMS) for which broadband data was extracted from the testbed database (filled blue inverted triangles). Data from the two broadband primary stations closest to the epicenter, NV32 and PD31 (open blue inverted triangles), were excluded because the interval stored in the waveform database was too short. Figure 4B shows the waveform fits and the moment tensor resulting from the automatic inversion of data filtered in a passband between 20 s and 50 s using Greens functions derived from the iasp91 velocity model. While the waveform fits do not look very bad, the moment tensor is the opposite of those given by the Harvard CMT and USGS catalogs and the total reduction in variance is only 18 percent. We investigated the waveforms and instrument information given for the four primary stations. It appears that the instrument response functions stored in the database for the stations ULM and IL31 have reversed polarity. Figure 4C shows the results for the same four stations, when the instrument response has been corrected. In addition, we have used a filter passband between 33 s and 100 s, more appropriate for the size of the Hector Mine earthquake, and less susceptible to the influence of lateral heterogeneity.. The new moment tensor result agrees well with the catalog results and the variance reduction is better than 50 percent. For Figure 4D we have added data from three auxiliary stations of the IMS network (filled red inverted triangles) to the inversion. The data for stations ANMO and CCH was extracted from the database of the Incorporated Research Institutions in Seismology (IRIS), while data from YBH came from the archives of the Berkeley Seismological Laboratory. The stations YBH and ANMO are approximately the same distance from the epicenter as PD31. This inversion shows how the auxiliary stations can supply data from locations close to the epicenter while improving the coverage of the focal sphere.

Figure 2 also shows the moment tensors calculated using the SW method (lower map). Again, the moment tensors calculated using modes derived from two velocity models, 1066b (blue, Gilbert and Dziewonski, 1975) and the PREM velocity model (green) can be compared with the moment tensors given in the Harvard CMT (brown) and USGS (red) catalogs. Fewer of the events selected from the catalog are present on this map than the upper map for the CW method. Moment tensors were calculated only for events if high quality, three-component data were available for more than 2 stations, that is data with no gaps, of a sufficient length between group velocities of 4.5 km/s and 2.0 km/s, and with a signal-to-noise ratio in power greater than 100. Figure 3C shows the moment tensor difference function comparing the results from the SW inversions using 1066b and PREM modes with Harvard CMT catalog moment tensors and with each other, while Figure 3D compares the calculated moments. While the mechanisms for some events agree well with the catalog values, for others, they are completely different. This is also apparent in the plot of the moment tensor difference function (Figure 3C), where it is clear that the results from the 1066b inversion are basically the same as those from the PREM inversion (plusses). Clearly, the values of the moments determined for these events are low, compared with the Harvard CMT catalog (Figure 3D), on average a factor of 7 lower. This is independent of the model used, as the average for the ratios of the moments determined using the 1066b model and PREM is about 1 (plusses).

Figure 5 shows the results of the surface wave inversion of the Hector Mine event (origin ID 20595122, 16 October 1999). The phase and amplitude fits are shown for all stations and frequencies used to produce the result given on the right hand side of the figure. Just as the reversed polarity of the instrument correction for stations ULM and IL31

affected the solution for the CW method, it will have an effect on the results of the surface wave method. We must determine which other stations may have similar problems. We are also investigating the cause of the low estimate of events' moments calculated in the course of the inversion.

CONCLUSIONS AND RECOMMENDATIONS

The automatic procedure to determine moment tensors has been implemented on the testbed at the Center for Monitoring Research. The procedure selects events from the reviewed event bulletin and calculates moment tensors, the events' depths and moments using the complete waveform and surface wave methods developed at U.C. Berkeley. Results from a set of earthquakes with $m_b > 5.4$ and depth shallower than 200 km that occurred between 19 July and 16 October 1999 demonstrate both the effectiveness of the procedure, as well as the areas where improvement is necessary. We have calculated the results of each method, the CW method and the SW method, using synthetic information calculated from two global velocity models. We are investigating solution differences that are apparently due to the choice of velocity model. Initial observations suggest that for the CW method, the differences in the automatic solutions usually result from incorrect alignment with the Greens function. When solutions are reviewed, and the alignment of the waveforms and the Greens function adjusted, the results are much more consistent for the two models.

One of the most basic problems we encountered in the development process relates to the amount and quality of the data used in the inversions. For the methods to function well, the waveform data must have a high signal-to-noise ratio and no gaps or glitches. In many regions of the world, for example the southwest Pacific Ocean, there are very few primary stations. The results of the inversion could be improved by using recordings from auxiliary stations of the IMS network equipped with broadband instruments. Unfortunately, for the test interval, it is impossible to go back and retrieve such data to add in to the inversion. We have been using recent events to test feasibility of using data from auxiliary stations in the moment tensor procedure. In practice, data from auxiliary stations are used in producing the REB, however, generally only very short intervals of data are requested from the stations. These intervals are not long enough to be useful for moment tensor inversions. We recommend that intervals starting at the event origin time and ending with the end of the surface wave train be requested from auxiliary stations with broadband instruments within 50 degrees of the event and stored in the waveform database for use with the moment tensor code. If it is not possible to handle the resulting volume of data, we suggest that at least 1 sps data be stored.

Recently, the Center for Monitoring Research has been collecting waveform data from earthquakes and nuclear explosions in and around Lop Nor as part of an advanced concept demonstration (ACD). Figure 6 shows a set of 175 earthquakes recorded between 1995 and 2002 as well as 25 nuclear explosions dating from 1966 to 1996. As an example of the calibration of the automatic moment tensor procedures for a specific region, we are planning to use this data along with the 3D velocity structure given by CUB1.0 (Anatolik *et al*, 2001). We will compare the moment tensor results with those determined by Bukchin *et al* (2001).

REFERENCES

Anatolik, M., G. Ekström, A. M. Dziewonski, L. Boschi, B. Kustowski, and J Pan (2001), Multi-Resolution Global Models for Teleseismic and Regional Event Location, *23rd Seismic Research Review: Worldwide Monitoring of Seismic Explosions*, Jackson Hole, WY, October 1-5.

Kukchin, B. G., A z. Mostinsky, A. A. Egorkin, A. L. Levshin, and M. H. Ritzwoller (2001), Isotropic and Nonisotropic Components of Earthquakes and Nuclear Explosions on the Lop Nor Test Site, China, *Pure Appl. Geophys.*, **158**, 1497-1515.

Dreger, D. and D. V. Helmberger (1991), Complex Faulting Deduced from Broadband Modeling of the 28 February 1990 Upland Earthquake (M_L=5.2), *Bull. Seism. Soc. Am.*, **81**, 1129-1144.

Dreger, D. and B. Romanowicz (1994), Source Characteristics of Events in the San Francisco Bay Region, *USGS Open-file report, 94-176*, 301-309.

Dreger, D. (1997), The Large Aftershocks of the Northridge Earthquake and their Relationship to Mainshock Slip and Fault Zone Complexity, *Bull. Seism. Soc. Am.*, **87**, 1259-1266.

Dreger D. and B. Woods (2002), Regional Distance Seismic Moment Tensors of Nuclear Explosions, *Tectonophysics*, in press.

Dreger, D. S., H. Tkalcic, and M. Johnston (2000), Dilational Processes Accompanying Earthquakes in the Long Valley Caldera, *Science*, **288**, 122-125.

Dziewonski, A. M., T.-A. Chou, and J. H. Woodhouse (1981), Determination of Earthquake Source Parameters from Waveform Data for Studies of Global and Regional Seismicity, *J. Geophys. Res.*, **86**, 2825-2852.

Dziewonski, A. M. and D. L. Anderson (1981), Preliminary Reference Earth Model, *Phys. Earth Plan. Int.*, **25**, 297-356.

Ekstrom, G., A. M. Dziewonski, and J. Steim (1986), Single station CMT:Application to the Michoacan, Mexico, Earthquake of September 19, 1985, *Geophys. Res. Lett.*, **13**, 173-176.

Fan, G. and T. Wallace (1991), The Determination of Source Parameters for Small Earthquakes from a Single, very Broadband Seismic Station, *Geophys. Res. Lett.*, **18**, 1385-1388.

Fukuyama, E., M. Ishida, D. Dreger, and H. Kawai (1998), Automated Seismic Moment Tensor Determination by Using OnLine Boadband Seismic Waveforms*, Jishin*, **51**, 149-156.

Fukuyama, E. and D. Dreger (2000), Performance Test of an Automated Moment Tensor Determination System, *Earth Planets Space*, **52**, 383-392.

Gee, L., D. Dreger, D. Neuhauser, R. Uhrhammer, and B. Romanowicz (1996), The REDI program, *Bull. Seism. Soc. Am.*, **86**, 936-945.

Gilbert, F. and A. M. Dziewonski (1975), An Application of Normal Mode Theory to the Retrieval of Structural Parameters and Source Mechanisms from Seismic Spectra, *Phil. Trans. Roy. Soc. Lon.*, **278**, 187-269.

Kennett, B. L. N. and E. R. Engdahl (1991), Traveltimes for Global Earthquake Location and Phase Identification, *Geophys. J. Int.*, **105**, 429-465.

Mendiguren, J. (1977), Inversion of Surface Wave Data in Source Mechanism Studies, *J. Geophys. Res.*, **82**, 889-894.

Müller, G. (1973), Theoretical Body Wave Seismograms for Media with Spherical symmetry; Discussion and Comparison of Approximate Methods, *J. Geophysics*, **39**, 229-246.

Müller, G. (1977), Earth-Flattening Approximation for Body waves Derived from Geometric Ray Theory; Improvements, Corrections and Range of Applicability, *J. Geophysics*, **42**, 429-436.

Pasyanos, M. (1996), Regional Moment Tensors and the Structure of the Crust in Central and Northern California, *Ph.D. Thesis, University of California, Berkeley*, 261p.

Pasyanos, M., D. Dreger and B. Romanowicz (1996), Toward Real-Time Estimation of Regional Moment Tensors, *Bull. Seism. Soc. Amer.*, **86**, 1255-1269.

Patton, H. J. (1988), Source Models of the Harzer Explosion from Regional Observations of Fundamental-Mode and Higher Mode Surface Waves, *Bull. Seism. Soc. Am.,* **78**, 1133-1157.

Pechmann, J. C., W. R. Walter, S. J. Nava, and W. J. Arabasz (1995), The February 3, 1995, ML 5.1 Seismic Event in the Trona Mining District of Southwestern Wyoming, *Seis. Res. Lett.*, **66**, 25-34.

Romanowicz, B. (1982), Moment Tensor Inversion of Long Period Rayleigh Waves: A New Approach, *J. Geophys. Res.*, **87**, 5395-5407.

Romanowicz, B. and Ph. Guillemant (1984), An Experiment in the Retrieval of Depth and Source Parameters of Large Earthquakes Using Very Long Period Rayleigh Wave Data, *Bull. Seism. Soc. Am.*, **74**, 417-437.

Romanowicz, B., M. Pasyanos, D. Dreger, and R. Uhrhammer (1993), Monitoring of Strain Release in Central and Northern California Using Broadband Data, *Geophys. Res. Lett.*, **20**, 1643-1646.

Saikia, C. (1994), Modified Frequency-Wavenumber Algorithm for Regional Seismograms using Filon's Quadrature: Modeling of Lg Waves in Eastern North America, *Geophys. J. Int.*, **118**, 142-158.

Stump, B. W., and L. R. Johnson (1984), Near-Field Source Characterization of Contained Nuclear Explosions in Tuff, *Bull. Seism. Soc. Am.*, **74**, 1-26.

Tajima, F., D. S., Dreger, and B. Romanowicz (2000), Modeling of the Transitional Structure from Ocean to Continent in the Mendocino Region using Broadband Waveform data, *EOS*, **81**, no. 48 (Fall meeting supplement).

Vasco, D. and L. Johnson (1989), Inversion of Waveforms for Extreme Source Models with Application to the Isotropic Moment Tensor Component, *Geophys. Journ. Royal Astr. Soc.,* **97**, 1-18.

Walter, W. R. (1993), Source Parameters of the June 29, 1992 Little Skull Mountain Earthquake from Complete Regional Waveforms at a Single Station, *Geophys. Res. Lett*., **20**, 403-406.

Table 1. Events of test interval, July 19 – October 16, 1999

OriginID	Date	Lat	Lon	Depth	m_b %	Region
20537870	1999 7 19 2:17:09.150	-28.561	-177.424	70	5.64	Kermadec
20541908	1999 7 26 1:33:15.178	-5.210	152.076	16	5.68	New Britain
20542430	1999 7 28 0:16:59.480	-28.606	-177.322	34	5.47	Kermadec
20542756	1999 7 28 10:08:18.210	-30.239	-177.774		5.81	Kermadec
20553840	1999 8 12 5:44:56.157	-1.595	122.667		5.56	Sulawesi
20555310	1999 8 14 0:16:54.100	-5.840	104.674	102	5.87	S. Sumatra
20559538	1999 8 17 0:01:37.795	40.772	30.092		5.59	Turkey
20560647	1999 8 20 10:02:18.146	9.260	-84.165		5.46	Costa Rica
20561207	1999 8 22 12:40:42.345	-16.095	168.213		5.94	Vanuatu
20568654	1999 9 7 11:56:49.481	38.161	23.544		5.50	Greece
20576492	1999 9 18 21:28:34.048	51.264	157.499	50	5.61	Kamchatka
20576889	1999 9 17 14:54:46.930	-13.815	167.446	169	5.72	Vanuatu
20577664	1999 9 20 17:47:29.732	23.548	121.012		5.94	Taiwan MS*
20577672	1999 9 20 17:57:19.559	23.852	121.217	43	5.42	Taiwan AS*
20578273	1999 9 20 18:11:50.377	23.811	121.136		5.83	Taiwan AS*
20578492	1999 9 22 0:14:42.005	23.747	121.091	33	5.45	Taiwan AS
20581262	1999 9 25 23:52:53.459	23.774	121.158	37	5.46	Taiwan AS
20582713	1999 9 29 4:42:55.319	1.907	125.195	158	5.37	Molucca Passage
20582842	1999 9 29 18:01:28.201	-30.763	-71.902		5.43	Central Chile
20583432	1999 9 30 16:31:09.188	16.083	-96.800		5.95	Oaxaca
20590301	1999 10 10 7:03:01.547	-1.960	134.100		5.48	W. Irian
20591829	1999 10 13 1:33:38.755	54.691	-161.136	13	5.54	Alaska Pen
20595122	1999 10 16 9:46:45.597	34.541	-116.361		5.35	Hector Mine

% Given in the testbed database

* No MT solutions determined due to data overlap

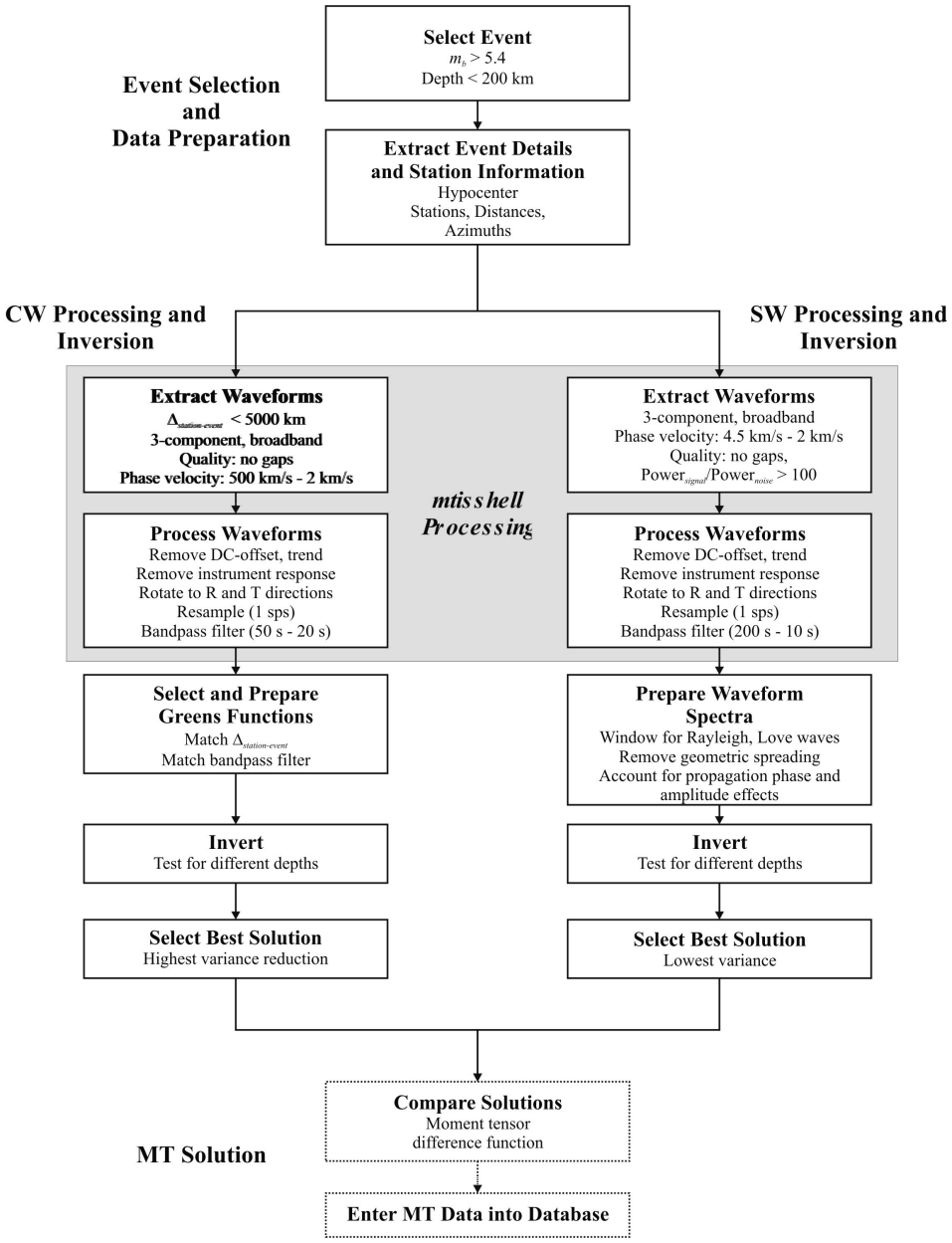

Figure 1. Flowchart describing the automated moment tensor data selection and processing procedure. Event selection parameters are given which characterize the events described in the following text.

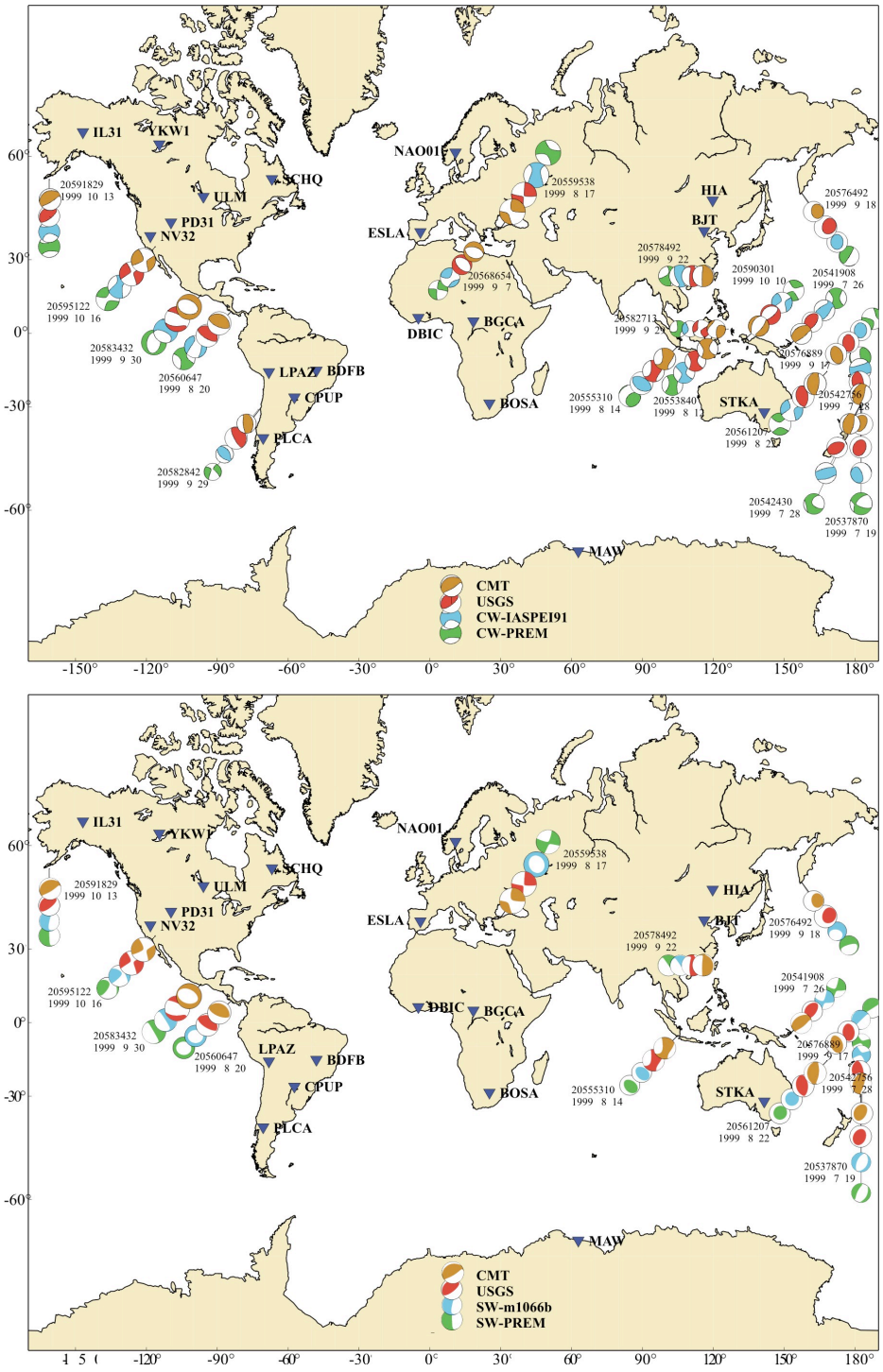

Figure 2. Maps showing the inversion results for the events of the test interval. Inverted triangles mark the locations of stations used in the inversions. The upper map compares results from the CW method using Greens functions based on the iasp91 **(blue) and the PREM (green) velocity models with moment tensors from the Harvard CMT (brown) and USGS (red) catalogs. The lower map compares moment tensors generated by the SW method using modes calculated from the velocity models 1066b (blue) and PREM (green) with those from the Harvard CMT (brown) and USGS (red) catalogs.**

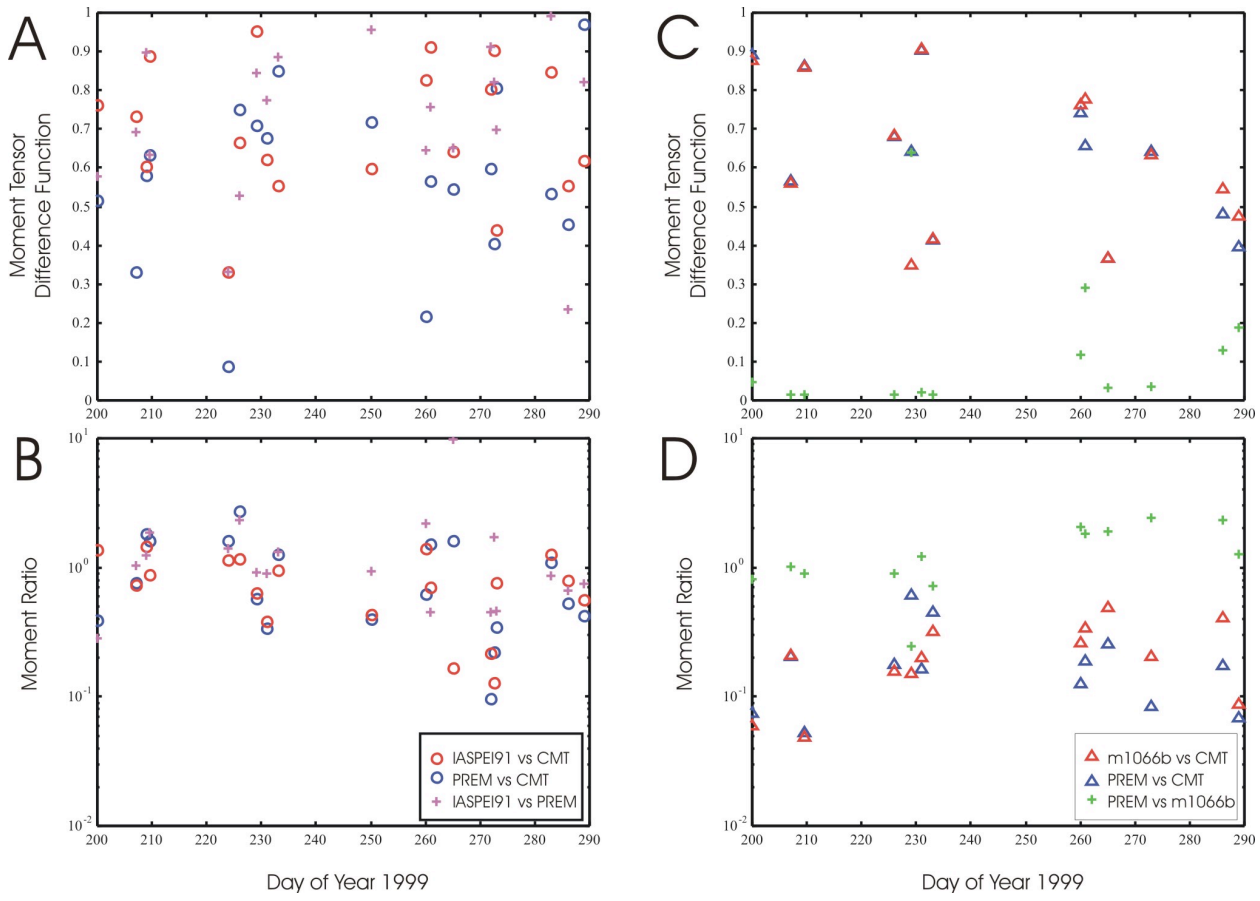

Figure 3. Quantitative comparison of moment tensor solutions from CW (A, B) and SW (C, D) with Harvard CMT results. A and C show the moment tensor difference function (Pasyanos *et al*, 1996). If the difference function is less than 0.5, the moment tensors are similar. B and D show the ratio between the moment of the event calculated using the various methods.

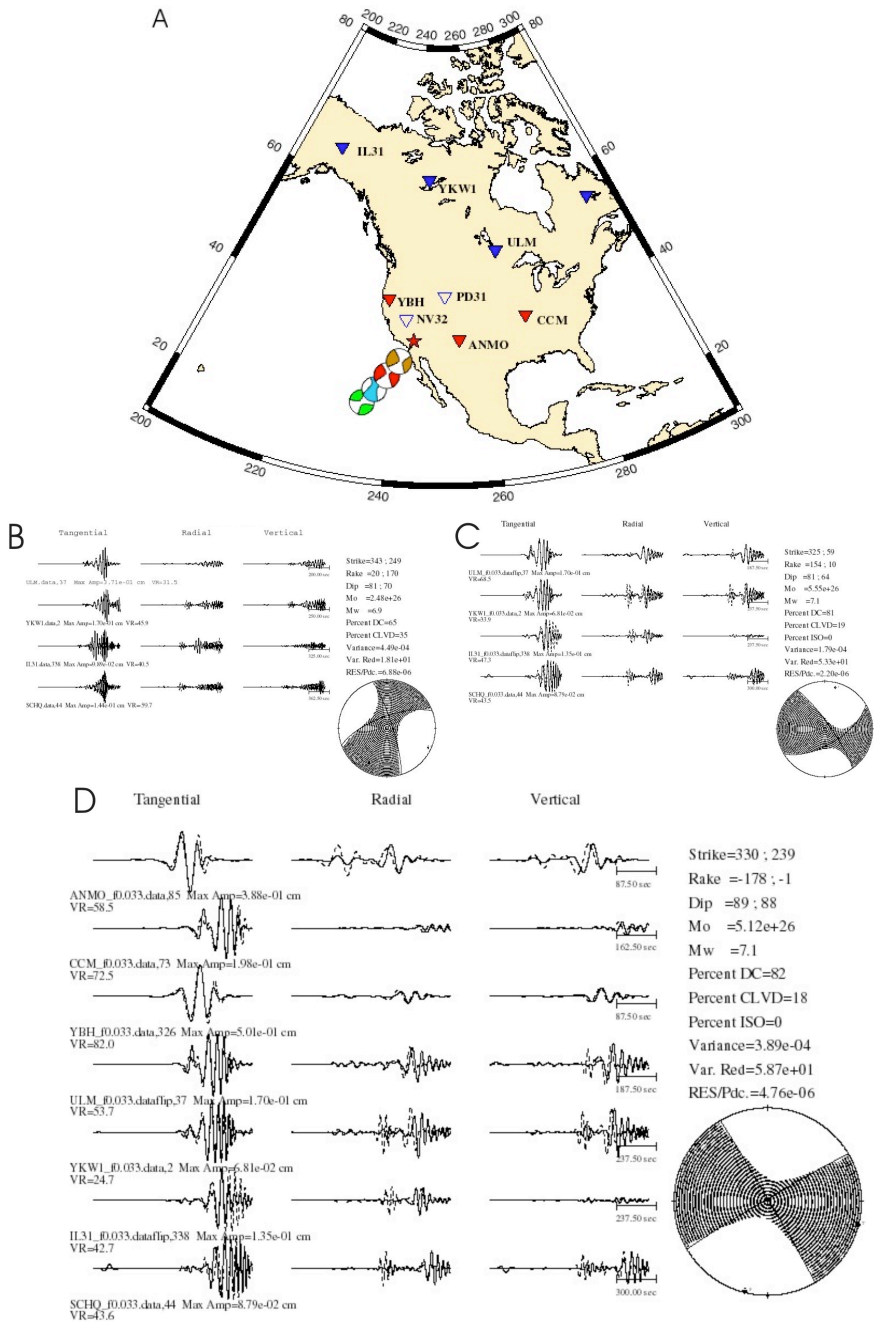

Figure 4. Complete waveform inversion of the Hector Mine event (origin ID 20595122, October 16, 1999). (A) The star shows the epicentral location. Data for the primary stations (filled blue inverted triangles) IL31, YKW1, ULM and SCHQ were extracted from the database. Data from primary stations (open blue inverted triangles) NV32 and PD31 were rejected as being too short. To improve and check the CW inversion, we requested data from the auxiliary stations (filled red inverted triangles) YBH, ANMO and CCM. This data was not available in the testbed database. The moment tensors are as given in Figure 2. (B) Automatic moment tensor solution. (C) Revised moment tensor solution. (D) Moment tensor solution including data from auxiliary stations. See text for discussion.

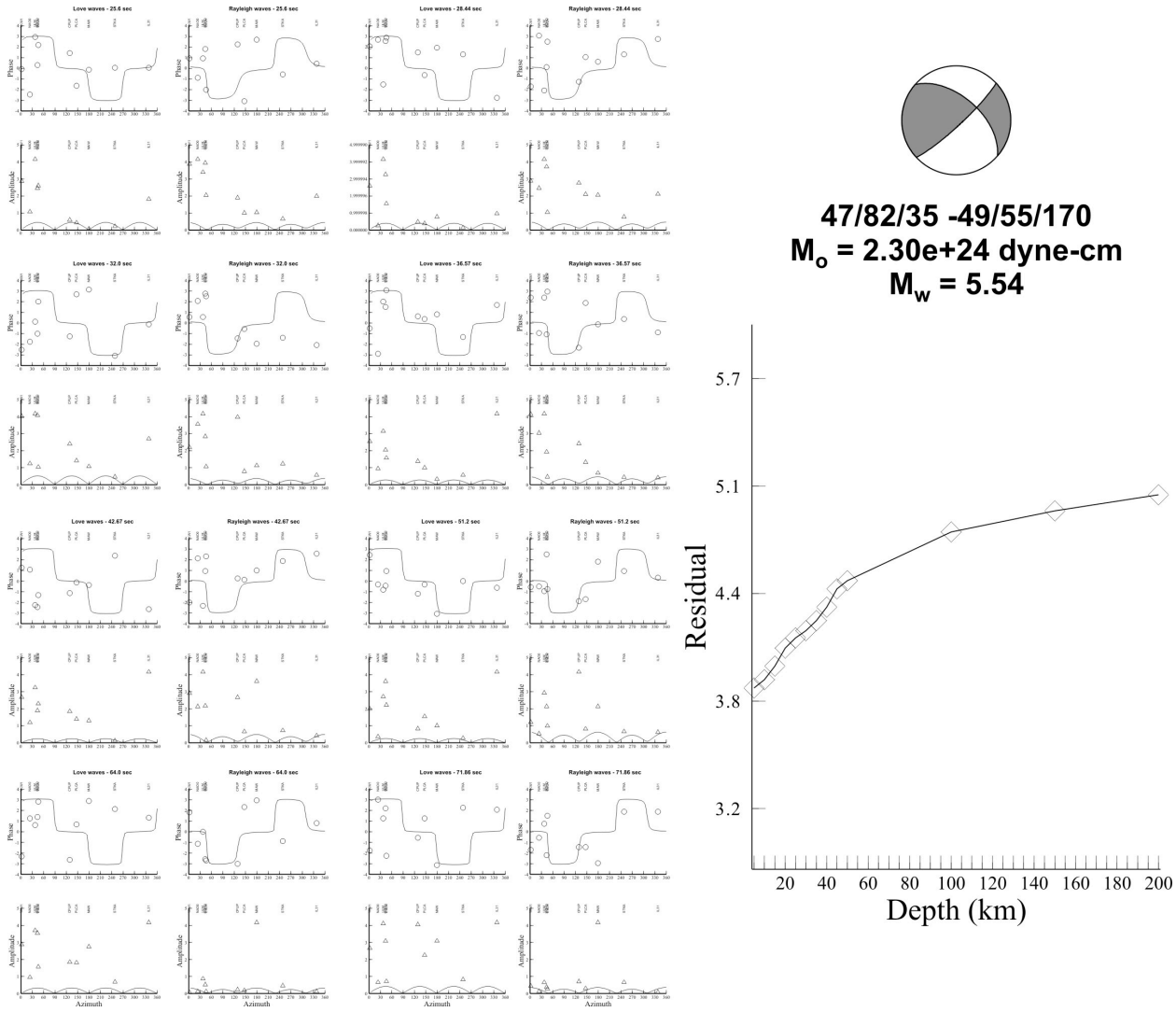

Figure 5. Surface wave inversion of the Hector Mine event (origin ID 20595122, October 16, 1999). The plots on the left show the phase and amplitude fits for the stations and frequencies used to generate the automatic solution. The plot on the right shows the source mechanism and the residuals. For this event, the best solution is found for a depth of 5 km, the shallowest depth used.

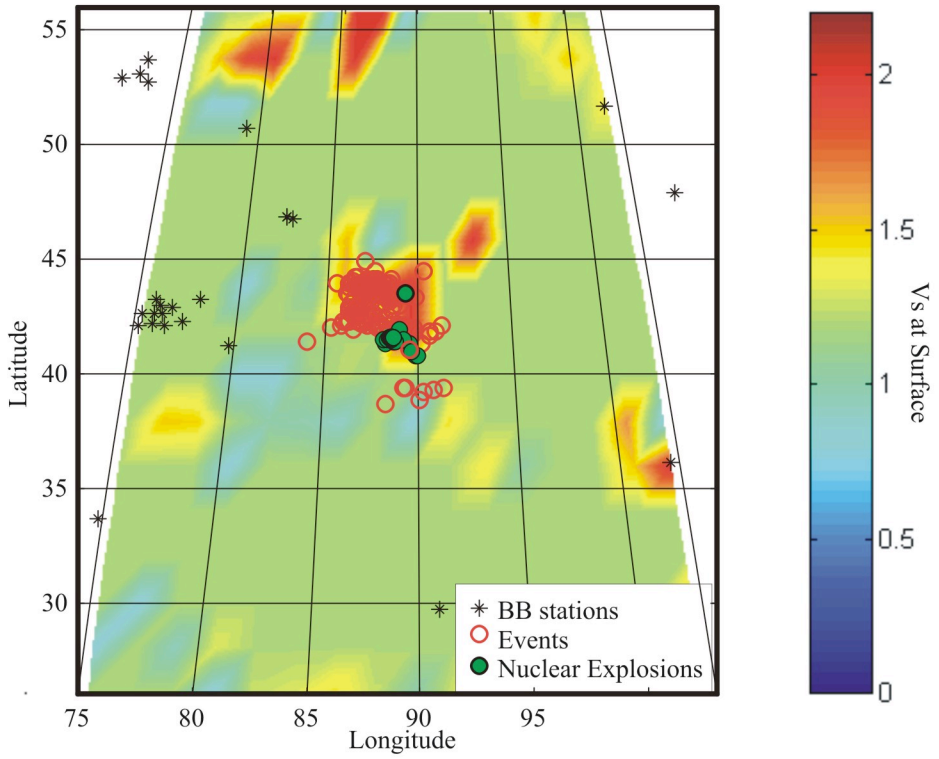

Figure 6. Lop Nor, the advanced concept demonstration region. Waveforms for 200 events, among them 25 nuclear explosions, have been collected for this region. The recordings come from 54 stations equipped with broadband instruments. The color map shows the S-wave velocity at the surface given by the model CUB1.0.